International Journal of Engineering Research and Technology. ISSN 0974-3154, Volume 14, Number 1 (2021), pp. 41-47

Studying the Effects of Partial Cavitation on the Rudder Force of the Vessel

Pham Ky Quang[1,*], Vu Van Duy[2], Trinh Xuan Tung[1], Nguyen Thi Lien[3]

[1]School of Excellent Education, Vietnam Maritime University, Vietnam.

[2]School of Mechanical Engineering, Vietnam Maritime University, Vietnam.

[3]Faculty of Economics, Vietnam Maritime University, Vietnam.

**Corresponding author: Pham Ky Quang; phamkyquang@vimaru.edu.vn*

Abstract:

The article aims to materialize the theory of propeller cavitation in order to build up a research model and a mathematical foundation that is used for simulated calculation bases on the CFD application. To demonstrate the simulation calculation, this research used the same rudder model with the rudder of M/V TAN CANG FOUNDATION, 420 TEUs and deployed the calculation for 56 different working points corresponding to the steering angle is 0^0, 5^0, 10^0,15^0, 20^0, 25^0, 30^0, 35^0 and the flow rate is 4.5, 5.0, 5.5, 6.0, 6.5, 7.0, 7.5 m/s, respectively. And from which the general point about the problem of cavitation on the rudder of the ship was formed. The period of partial cavitation that occurs on the rudder will be paid particular attention to study how it affects the rudder force. In practice, the instability of the rudder force might be caused by a number of factors such as the synchronized effects of free surface and the propeller rotation, the external effects, the impact of cavity bubbles caused by the propeller. Moreover, the periodical appearance of the partial cavitation directly affects the rudder force by creating an oscillation with a specified period and amplitude. To solve the above-mentioned problems, the authors built up a system of experiments that using a propeller model is similar to the rudder of M/V TAN CANG FOUNDATION, 420 TEUs. The results of these experiments illustrate that what the consequences of rudder cavitation are and how it affects the rudder force when partial cavitation occurs on the rudder.

Keywords: CFD, propeller, rudder cavitation, rudder force, vessel.

I. BUILDING THE MODELS INTRODUCTION

The rudder is a controlling object to alter the course of a vessel. Because of being fitted behind the propeller in order to convert the energy of flow into the rudder force, physical phenomena related to energy exchange between the rudder and the behind-propeller flow create remarkable impacts on the rudder force.

One of the popular phenomena is rudder cavitation which is quite complicated and has obvious effects on the rudder force, especially in situations a vessel has to change the telegraph frequently such as maneuvering, sailing at high speed...

Figure 1: Illustrating cavity spots on the rudder (rudder of M/V TAN CANG FOUNDATION in periodical repair at Ship Marine shipyard, May 2017)

There are many published studies on rudder cavitation, the propeller cavitation such as the experimental research and simulated calculation regarding the "semi spade" rudder cavitation [1].

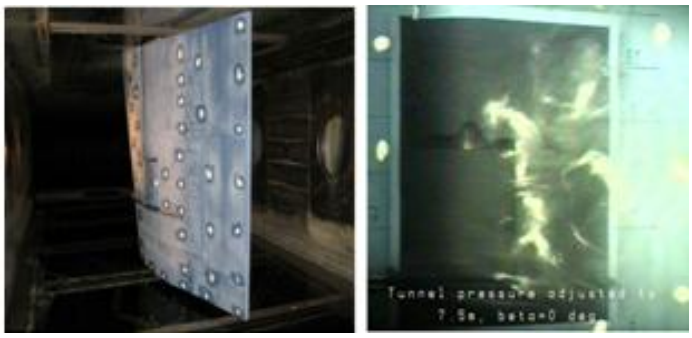

Figure 2: Picture of cavitation on the rudder in the HYKAT experiment system, Germany

Obviously, the problem of rudder cavitation significantly affects the structure of the rudder. However, within the scope of this research, the influence of local erosion on the steering force in the process of cavitation was studied by applying Boundary Element Method (BEM) to calculate pocket slightly aggressive for each rudder profil, then connect to form a full airbag on the rudder. This study combined with the

application of Fluent-Ansys software to calculate the same rudder model and expand the problem to determine the period of cavitation as well as the steering force acting on the ship's rudder.

II. BUILDING A STUDY MODEL AND MATHEMATICAL FOUNDATION

II.I. Study model

The authors built up a study model by using the "mixture" problem, illustrated in Fig 3 [2-9].

Where:

- *V* is the ship's advanced velocity
- *Input 1* is the liquid phase, represents the flow behind propeller covers rudder (*V*);
- *Input 2* is the liquid phase, represents the velocity of the flow behind the propeller (*1.3V*) [5,10-11].

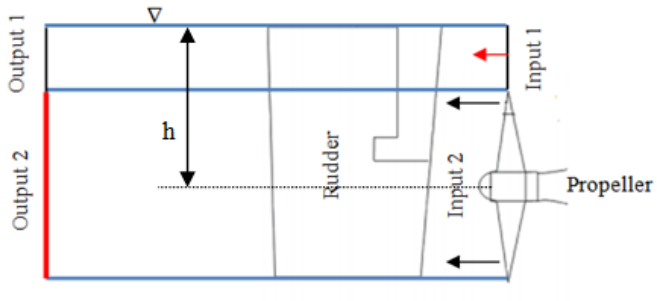

Figure 3: Building up the study model

The profile at the rudder's center shows the depth at which the rudder is fitted. Besides, the input of the problem is the geometric boundary configuration of the rudder, the rudder angle. Other conditions of the boundary are selected to diminish effects on the features of the problem (converting the energy of the flow into the rudder force acting on the rudder).

II.II. Mathematical foundation

The mathematical foundation has been widely studied [5,12-14]. In this article, the authors used two methods, the first - the Boundary Element Method (BEM) for the problem of the flow around the profile and the latter - the Finite Volume Method. Only non-compressed and continuous liquid is studied.

Where:

U_∞ is the velocity of the inflow (m/s);

α is the rudder angle (degree);

D is the starting point of the cavity area;

L is the last spot of the blade profile;

l is the length of the cavitation region;

λ is coefficient;

E is a point on the *Sc*, the starting point of the converting region with the length of λ_l.

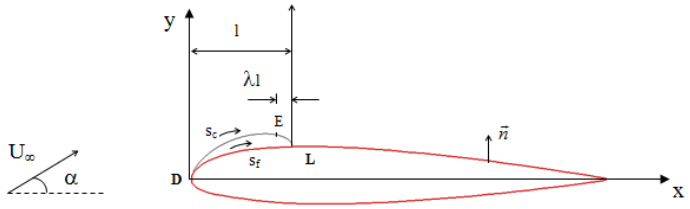

Figure 4: Illustrating the BEM method for the rudder's profile

In the cavity region, pressure (p_c) is the steam saturated pressure of the liquid (P_{bh}), which means:

$$p_c \leq p_{bh} \tag{1}$$

Condition of the kinematic boundary on the area of cavitation should satisfy the following equations:

Cavitation number:

$$\sigma = \frac{p_1 - p_{bh}}{\frac{1}{2}\rho V_1^2} \tag{2}$$

Velocity in the cavity area:

$$V_c = U_\infty \sqrt{1+\sigma} \tag{3}$$

Velocity in the transition area λ_l, calculated as following:

$$V_{tr} = U_\infty \sqrt{1+\sigma}\left[1 - f\left(S_f\right)\right] \tag{4}$$

with function $f(_{sf})$ is defined in Equation (5).

$$f(s_f) = \begin{cases} 0, & khi\ s_f < s_E \\ A\left(\frac{s_f - s_E}{s_L - s_E}\right)^v & khi\ s_e \leq s_f \leq s_L \end{cases} \tag{5}$$

Where:

S_f is the length of chord of blade (m);

value of S_E, S_L are mentioned in Fig 4, measured from the edge of the blade;

A ($0 < A < 1$) and ν ($\nu > 0$) are the optional constants.

The closing condition of the vapor region on the profile of the blade:

$$h(s_L) = 0 \tag{6}$$

This means the height of the vapor region at the closing point on the *L* blade is 0.

Conclude: From the model of this problem and the conditions of the boundary configuration of the blade profile and in the cavity area, the dimensions of the vapor region could be

calculated as the following procedures.

- Divided the blade boundary configuration into *N* panel:

$$N = N_c + N_w \tag{7}$$

Where:

N_c is the number of panels in the cavity area;

N_w is the number of remained panels.

p is selected as the original point, according to the Green theorem, it will be obtained:

$$\pi\phi_p = \int_s \left(-\phi \frac{\partial \ln r}{\partial n} + \frac{\partial \phi}{\partial n} \ln r \right) ds - \int_w \Delta\phi_w \frac{\partial \ln r}{\partial n} ds \tag{8}$$

Where:

ϕ_p is perturbation potential at the original point "O";

r is the distance from O (X_O, Y_O) to *ds* elements that are along with the profile boundary configuration in the cavity area and the free cavity area;

$\Delta\phi w$ is the pitch of the potential jump at the edge of the next blade;

S_c is the length of the chord of the cavity area (refer to Fig 4).

then:

$$\frac{\partial \phi}{\partial S_c} + \frac{\partial \Phi_{in}}{\partial S_c} = V_c \left[1 - f\left(S_f\right) \right] \tag{9}$$

and the surface potentials of the cavity area is calculated as the following:

$$\phi(S_c) = \phi(0) - \Phi_{in}(S_c) + \Phi_{in}(0) + V_c \int_0^{s_c} \left[1 - \left(S_f\right) \right] ds \tag{10}$$

Hence, the loops are carried out to maintain the closing conditions on the blade profile. This means that length "*l*" and height "*h*" of the vapor region could be changed, with the given cavitation factors to satisfy the closing condition as the below:

$$h(s_L) = \frac{1}{V_c} \int_0^{s_{cL}} \left[\vec{U}_\infty \vec{n} + \frac{\partial \phi}{\partial n} \right] ds = 0 \tag{11}$$

Where:

S_{cL} is the total length of the chord of the cavity surface or obtained as in the following expression:

$$\int_0^{s_{cL}} \frac{\partial \phi}{\partial n} \frac{ds_c}{1 - f\left(s_f\right)} = -\int_0^{s_{cL}} \frac{\partial \Phi_{in}}{\partial n} \frac{ds_c}{1 - f\left(s_f\right)} \tag{12}$$

With each given cavitation number (or the length of the cavitation area) and the corresponding sweepback, it is necessary to assign the position of detaching from the surface $l_{D/c}$, to implement loops to determine the closing point *L* and the shape of the vapor region by the following technic:

Assuming the height of the vapor region at any spot is δ, depending on l và σ (the length of the profile and the cavitation number).

$$\delta(l,\sigma) \equiv h_c(s_{cL}) = \frac{1}{V_c} \int_0^{s_{cL}} \left[\frac{\partial \Phi_{in}}{\partial n} + \frac{\partial \phi}{\partial n} \right] \frac{ds_c}{1 - f(s_f)} \tag{13}$$

Implementing loops with the provision that meets the closing conditions on the blade boundary configuration is $\delta(l,\sigma) = 0$. In this case, the cavitation factor is assigned, the loops are carried out by applying the "secant" method of Newton – Raphson [15].

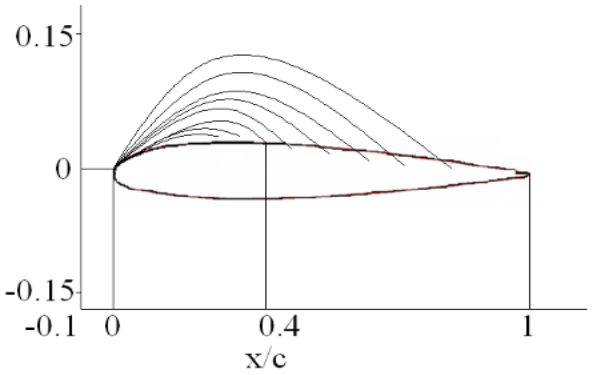

Figure 5. The doing loops to find the boundary configuration of the vapor region and closing spot *L*

The converging problem gives the positions of a closing point on the boundary configuration of the blade and the configuration of the vapor region, then other characteristics including C_p, C_L, C_m … could be obtained (refer to Fig 5).

The program that is written in Fortran programming language with a variety of profiles, rudder angles, and cavitation factors, will give the output consisting of the shape of the cavity vapor region and the chart of pressure distribution on the corresponding boundary configuration of the blade.

The mathematical foundation of the limited volume method: is published by many authors and is illustrated by the following steps [6,16]:

- Discretizing the calculating space by dividing into a grid;
- Solving the major differential equations such as Navier – Stokes, momentum, continuous, and energy equation to define the basic values such as velocity, pressure, specific gravity,…;
- Using these values in the phase transition equation to determine the ratio of the vapor state weight f_{vap}.

$$\frac{\partial}{\partial t}\left(\rho . f_{vap}\right) + \frac{\partial}{\partial x_j}\left(\rho . f_{vap} . u_{vap_j}\right) = \frac{\partial}{\partial x_j}\left(\gamma . \frac{\partial f_{vap}}{\partial x_j}\right) + R_e - R_c \tag{14}$$

Where:

R_e, R_c - depends on values of static pressure "*p*" and saturated steam pressure "p_{vap}".

- If $p < p_{vap}$: $R_e = C_e \frac{v_{ch}}{\sigma} \rho_l \rho_{vap} \sqrt{\frac{2(\rho_{vap}-\rho)}{3\rho_l}} (1 - f_{vap})$ (15)

- If $p > p_{vap}$: $R_c = C_c \frac{v_{ch}}{\sigma} \rho_l \rho_l \sqrt{\frac{2(\rho-\rho_{vap})}{3\rho_l}} f_{vap}$ (16)

Where:

v_{ch} is the typical velocity;

C_e, C_c is the experimental research constants, respectively (C_e = 0.02; C_c = 0.01) [15].

Hence, the results of the calculations will facilitate the determination of the percentage of vapor state in the entire calculating space leading to locating exactly the cavitation on the rudder. Especially, the calculating results based on time prove that the instability of the partial cavitation exists. This is a very fundamental factor to evaluate the effects of the partial cavitation on the rudder force.

III. RESULT ANALYSIS

III.I. Determining the period, frequency of cavity vapor region

The simulated calculation for each profile can determine whether the rudder is cavitated or not? If it is, what types of cavitation is it? What its characteristics are? In case cavitation appears, simulated calculation over time (with appropriate steps) is carried out to observe the process of formation, development, and disappearance of the part cavity vapor region, thence the period and frequency of oscillation could be obtained. This is also the oscillation frequency of the rudder force when the effects of the partial cavitation are taken into account.

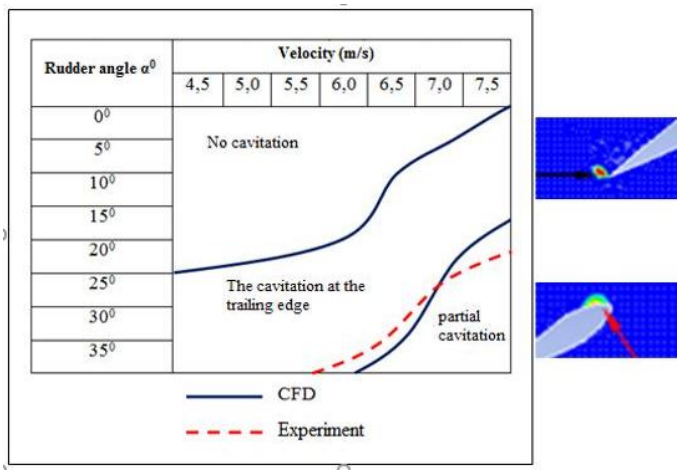

Figure 6: Summarize inputs at which cavitation occurs on the rudder of M/V TAN CANG FOUNDATION

By calculating different inputs of the rudder of M/V TAN CANG FOUNDATION, cavitation can be categorized as the cavitation at the trailing edge and the partial cavitation at the leading edge.

The input of cavitation appearing on the rudder is summarized in Fig 6 [5]. By applying CFD combined with experimental research, it figures out that the combined input of the propeller rotation and the rudder angle in which the cavitation on the rudder occurs, the cavitation at the trailing edge as well as the partial cavitation at the leading edge appears (in these cases, the revolution of propeller is converted into the velocity of the rudder around flow V (m/s)).

Results of the simulated calculation in the specified case: the rudder angle α = 30^0 and the velocity of the flow around rudder V = 7.5 m/s illustrated in Fig 7 [5].

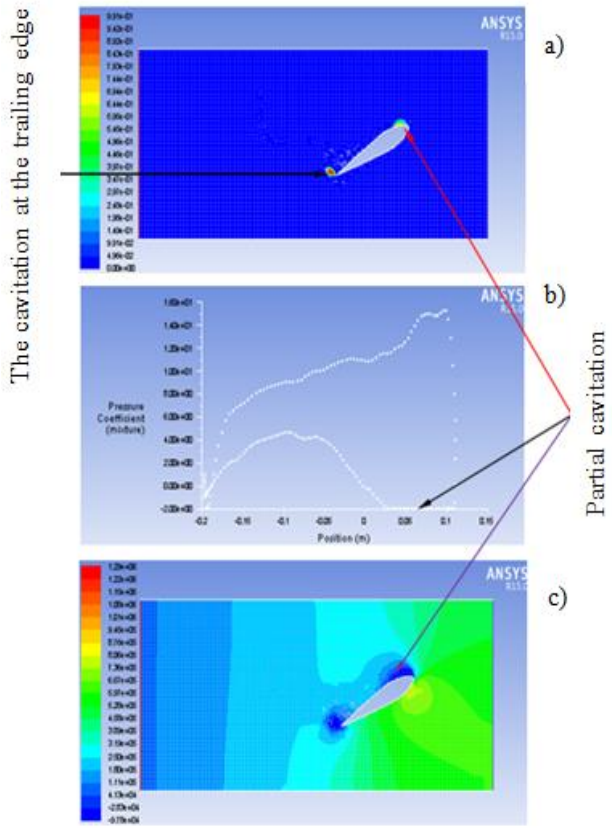

Figure 7: Results of the simulated calculation of cavitation on the profile at $\alpha = 30^0$; V = 7.5 m/s

By looking at Fig 7, it can be seen that:

- Fig 7a indicates the distribution of vapor state in the calculating space and figures out that the area has the vapor phase is approximate 100% (the cavity vapor region) at the leading edge of the rudder (known as the partial cavitation) [5,11] and the cavitation at the trailing edge;
- Fig 7b presents the pressure on the profile which means the length of the partial cavity area on the profile is the horizontal line lying on the horizontal axis.
- Fig 7c illustrates the distribution of pressure in the calculating space with specified values and figures out the spots on which the cavitation at the leading edge and the trailing edge of the rudder occurs.

III.II. Determining the amplitude of oscillation of the rudder force on the rudder

In reality, the formation of the partial cavitation usually occurs only on some parts, not the entire rudder. Details are illustrated in Fig 8.

Where:

L is the height of the rudder (m);

k is the height of the partial cavitation region (m).

Hence, the amplitude of the rudder force of oscillation is fully achieved and is illustrated in Fig 9.

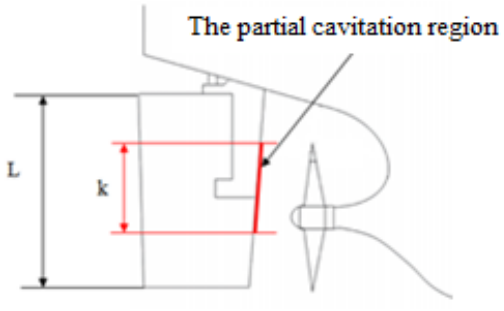

Figure 8: Illustrating a part of the stage of forming the partial cavitation on the rudder

The average rudder force R_{tb} is calculated as below:

$$R_{tb} = \frac{1}{4}(C_{Lmin} + C_{Lmax})\rho A_R V^2 \quad (17)$$

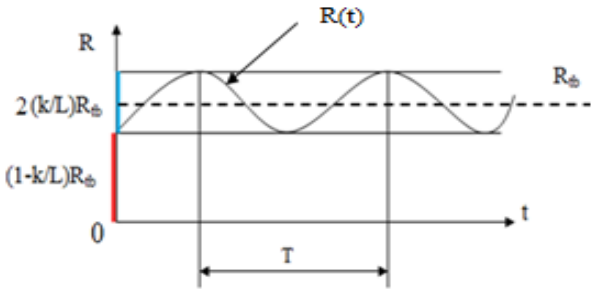

Figure 9: Rudder force when the partial cavitation occurs

In other cases of partial cavitation, results are shown as below:

- The periods of oscillation are the same value and approximate 0.091s.
- The amplitudes of oscillation C_L are shown the Table 1.

Table 1: Results of value C_L

Rudder angle α^0	Lift force factor C_L	Rudder angle α^0	Lift force factor C_L
20^0	0 ÷ 0.950	30^0	0 ÷ 2.191
25^0	0 ÷ 1.643	35^0	0 ÷ 2.298

In Fig 9, it is shown that the effects of the partial cavitation on the rudder force can be expressed through the oscillating period and the oscillating amplitude of the rudder force (in the stage of forming the partial cavitation on the rudder).

The period and amplitude of the oscillation (f) do not depend on the rate of turning rudder as well as the rudder angle but on the type of profile using to create a rudder. According to the calculations applying to the profile of the rudder of M/V TAN CANG FOUNDATION, the value of T and f are 0.091s and 11Hz, respectively.

The amplitude of oscillation depends on the velocity of flow and the rudder angle, shown in the following equation:

$$A = 2\frac{k}{L}R_{tb} \quad (18)$$

Where:

- R_{tb} is obtained as Equation (17);

- L is the height of the rudder (m), is calculated according to the part of the rudder covered by the flow;

- k is the part of the rudder on which partial cavitation appears, depending on the type of profile, rudder angle, the velocity of flow.

The simulated calculation for the 3D problem based on Fluent - Ansys software is carried out to obtain value "k" for the rudder of M/V TAN CANG FOUNDATION corresponding to either the velocity of the flow around the rudder and the values of rudder angle. The results of this calculation are expressed as a percentage of vapor phase distribution, shown in Fig 10.

By analyzing results in Fig 10, it shows that:

- In Fig 10a: the trail of cavity bubbles has the maximum vapor state of 62% (shown at the colored column on the left side of the picture) and occupies a relatively small area (the partial cavitation has not formed yet), k = 0 in this case which means that the rudder force is not effected dramatically by the partial cavitation.

- In Fig 10b: The maximum vapor state is 99% and the partially cavity vapor region is formed at the leading of the rudder, the ratio between the length k and the entire length of the rudder is $\frac{k}{L} = 0.187$, hence the rudder force that is affected by the partial cavitation can be calculated as the following:

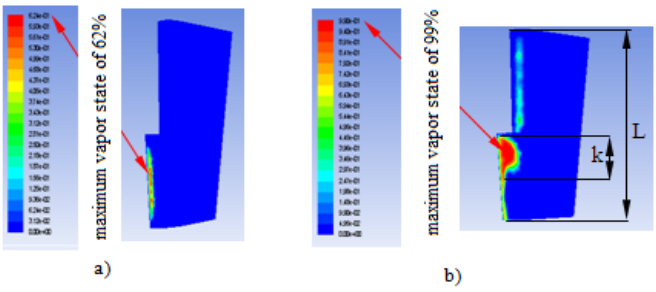

Figure 10: Results of calculating simulation of the percentage of vapor state on the rudder M/V TAN CANG FOUNDATION in case of V = 7.5 m/s and α = 15^0 (a), $\alpha = 35^0$ (b), respectively

The periods of oscillation are the same $T \approx 0.091$s.

The amplitudes of oscillation of C_L shown in Table 1 are 0 ÷ 2.298.

The average rudder force is:

$$R_{tb} = \frac{1}{4}(C_{Lmin} + C_{Lmax})\rho A_R V^2 = 387818.6\ N$$

with the rudder of M/V TAN CANG FOUNDATION has value $A_R = 12$ m^2, then:

The fluctuation of the rudder force:

$$A = 2\frac{k}{L}R_{tb} = 145044.1564\ N$$

The rudder force of the rudder area which is non-cavitation (R_o):

$$R_o = \left(1 - \frac{k}{L}\right)R_{tb} = (1 - 0{,}187) \times 387818.6 = 315296.5218N$$

The rudder force over time is illustrated in Fig 11.

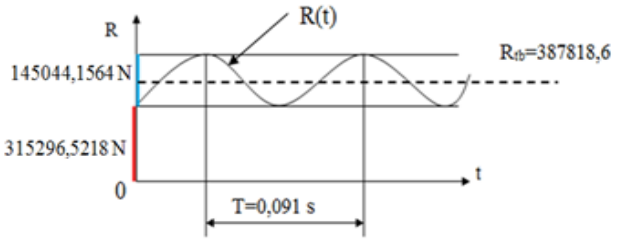

Figure 11: Illustrating the rudder force of M/V TAN CANG FOUNDATION in case $\alpha = 35^0$ and $V = 7.5$ m/s

IV. CONCLUSION

The article has achieved the following results:

- To concretize the theoretical basis of cavitation on the ship's rudder, including cavitation at the trailing edge and the partial cavitation at the leading edge. Besides that, this research formed a general point of the problem of cavitation on the rudder of the M/V TAN CANG FOUNDATION during the operation;
- Analyzed the effect of partial cavitation on the steering force, there was the partial cavitation on the rudder that caused oscillation with a certain frequency and amplitude, which depend on the rudder's profil and combination of (n_i, α_i);
- Calculated and simulated a specific simulation cycle and amplitude of the steering force impacting on the rudder of M/V TAN CANG FOUNDATION when $V = 7.5$ m/s and $\alpha = 35^0$.

ACKNOWLEDGMENTS

The authors would like to thank all colleagues in Vietnam Maritime University for assistance during the work. Additionally, we appreciate the constructive suggestions of the anonymous reviewers, which are invaluable in improving the quality of the manuscript.

REFERENCES

[1] L. Thomas, H. Streckwall, Cavitation Research on a Very Large Semi Spade Rudder, First International Symposium on Marine Propulsors, Trondheim, Norway, 2009. https://www.marinepropulsors.com/proceedings/2009/TA4-2-Lucke%20-%20Cavitation%20Research%20on%20a%20Very%20Large%20Semi%20Spade%20Rudder.pdf

[2] D.M. Andrea, G. Dubbioso, R. Muscari, M. Felli, CFD Analysis of Propeller-Rudder Interaction, Proceedings of the Twenty-fifth International Ocean and Polar Engineering Conference, Kona, Big Island, Hawaii, USA, 2015. https://www.researchgate.net/publication/280147383_CFD_Analysis_of_Propeller-Rudder_Interaction.

[3] S. Berger, M. Scharf, U. Gottsche, J.C. Neitzel, R. Angerbauer, M. Abdel-Maksoud, Numerical Simulation of Propeller-Rudder Interaction for Non-Cavitating and Cavitating Flows Using Different Approaches, Fourth International Symposium on Marine Propulsors smp'15, Austin, Texas, USA, 2015. https://www.semanticscholar.org/paper/Numerical-Simulation-of-Propeller-Rudder-for-and-Berger-Scharf/04c7a58180ed8ac85cda20c83251814513162a13.

[4] L. He, S.A. Kinnas, Numerical simulation of unsteady propeller/rudder interaction, International Journal of Naval Architecture and Ocean Engineering, 9(6), 2017, 677-692. https://doi.org/10.1016/j.ijnaoe.2017.02.004

[5] J.P. Breslin, and P. Andersen, Hydrodynamics of Ship Propellers, (Cambridge University Press, 2010), https://doi.org/10.1017/CBO9780511624254.

[6] S. Lee, K.J. Paik, Urans Simulation of a Partially Submerged Propeller Operating under the Bollard Condition, Brodogradnja, 69(1), 2018, 107-121. DOI: 10.21278/brod69107

[7] L.C. Nho, P.K. Quang, V.V. Duy, B.V. Cuong, C.T.A. Vu, N.T.N. Lai, Calculation and simulation of the current effects on maritime safety in the Haiphong fairway, Vietnam, The 17th International Association of Maritime Universities (IAMU) Annual General Assembly (Haiphong, Vietnam), 2016, 170 - 179, http://csum-dspace.calstate.edu/handle/10211.3/208088.

[8] C. Wang, S. Sun, L. Li, L. Le, Numerical prediction analysis of propeller bearing force for full-scale hull–propeller–rudder system, International Journal of Naval Architecture and Ocean Engineering, 8(6), 2016, 589-601. https://doi.org/10.1016/j.ijnaoe.2016.06.003

[9] K. Zelazny, Approximate Method of Calculating Forces on Rudder During Ship Sailing on a Shipping Route, The International Journal on Marine Navigation and Safety of

Sea Transportation, 8(3), 2014, 459-464.DOI: 10.12716/1001.08.03.18

[10] C. John, D. Radosavlijevic, S. Whitworth, Rudder – Propeller – Hull Interaction: The Results of Some Recent Research, In-Service Problems and Their Solutions, First International Symposium on Marine Propulsors, Trondheim, Norway, 2009. https://openaccess.city.ac.uk/id/eprint/15022/.

[11] K.J. Rawson, E.C. Tupper, Basic ship theory, 5th Edition, Publisher: Butterworth-Heinemann, 2001. ISBN: 9780750653985. https://doi.org/10.1016/B978-0-7506-5398-5.X5000-6.

[12] J. Carlton, Marine Propellers and Propulsion, 2nd Edition, Publishing Butterworth-Heinemann, 2007.

[13] S. Natarajan, Computational Modeling of Rudder Cavitation and Propeller/Rudder Interaction, Environmental and water resources engineering department of civil engineering, Report No.03-5, the University of Texas at Austin, 2003.

[14] P. Roger, Handbook of Computational Fluid Mechanics, Publisher: Academic Press, 1996. ISBN: 978-0-12-553010-1. https://doi.org/10.1016/B978-0-12-553010-1.X5000-2.

[15] A.K. Spyros, A.F. Neal, A numerical nonlinear analysis of the flow around two-and three-dimension partially cavitating hydrofoils, Journal of Fluid Mechanics, 254, 1993, 151-181. https://doi.org/10.1017/S0022112093002071

[16] L.Z. Wang, C.Y. Guo, Y.M. Su, T.C. Wu, A numerical study on the correlation between the evolution of propeller trailing vortex wake and skew of propellers, International Journal of Naval Architecture and Ocean Engineering, 10(2), 2018, 212-224. https://doi.org/10.1016/j.ijnaoe.2017.07.001.